THE EUROPEAN
PHYSICAL JOURNAL C

Barrow holographic dark energy: a path to reconstructing $f(R, T)$ gravity

P. S. Ens[a] ⓘ**, A. F. Santos**[b] ⓘ

Programa de Pós-Graduação em Física, Instituto de Física, Universidade Federal de Mato Grosso, Cuiabá, Brasil

© The Author(s) 2024

Abstract In this paper, we investigate one of the established methods for reconstructing modified gravity models from a dark energy model, with the aim of discovering relationships between these theories. In this study, we focus on the $f(R, T)$ modified gravity theory, where R denotes the Ricci scalar and T represents the trace of the energy–momentum tensor. We employ Barrow's holographic dark energy model, derived from fractal surfaces of black holes, to investigate the reconstruction process. The numerical results are subsequently presented for various infrared cutoffs, such as the Hubble horizon, future event horizon, and Granda–Oliveros cutoff.

1 Introduction

One of the most important discoveries in the last few decades is the late accelerated expansion of the universe, challenging the theory of general relativity and its extensive tests. The attempts made to explain this phenomenon have given birth to a vast set of propositions, many of them seeking ways to modify or add possibly missing parts to general relativity. Some consider the possibility of an energy permeating space, called dark energy, with extraordinary characteristics such as negative pressure and non-conservation. The most well-known candidate for dark energy is the cosmological constant, which induces an exponentially accelerated expansion. Considering an isotropic and homogeneous universe filled with this energy and dark matter, one arrives at the ΛCDM cosmological model. Although general relativity and the ΛCDM model are adequate to explain most of the observed phenomena [1], they do not offer a satisfactory explanation for the universe's expansion, since it is known that it does not evolve exponentially and varies over different epochs. Since constant dark energy cannot reproduce such observations, there has been an extensive search for dynamic forms.

One possibility for dynamic dark energy is adopted from the holographic principle [2,3], which is used to describe black hole thermodynamics [4–7]. This theory aims to study systems based on the characteristics of their boundaries. This concept can be applied to the universe as a whole, derived from the dynamics of a defined infrared cutoff. Here, a form of holographic dark energy is adopted from the idea of event horizons with fractal structures proposed by Barrow [8–10]. New equations of motion emerge from the presence of this energy, which we solved numerically for different infrared (IR) cutoffs: the Hubble radius, the future event horizon, and the Granda–Oliveros cutoff. Some of the constraints for this model are discussed in [11,12]. A similar study has been conducted on Tsallis holographic dark energy in [13]. Barrow dark energy has also been studied in the context of thermodynamics in [14–16].

In addition to considering an unobserved dark entity, some believe that general relativity needs corrections that would explain the expansion of the universe and are only relevant on cosmological scales. One way to achieve such corrections is by modifying the Lagrangian density that describes general relativity. In general relativity, the Lagrangian is proportional to the Ricci scalar, R. The most common and straightforward proposal for modification involves making the Lagrangian a function $f(R)$ [17], which may include non-linear terms. Taking it a step further, some theories introduce an additional level of interaction between curvature and the universe's components, leading to modifications such as $f(R, T)$, where T represents the trace of the energy-momentum tensor. Reviews on $f(R, T)$ modified gravity can be found in [18–24].

Many models of dark energy and modified gravity offer intriguing results and can solve some observed problems.

⌂ Springer

However, they often create new issues such as unrealistic fine-tuning and instabilities. These positive and negative characteristics can be found across various models, even among different concepts such as dark energy and modified gravity. It is possible to relate both concepts through their equations of state (EoS). A reconstruction of some $f(R, T)$ models from Bekenstein–Hawking holographic dark energy is presented in [25]. An analytical solution for the reconstruction of two $f(R, T)$ models, relating their effective state parameters to those of Tsallis holographic dark energy [26], considering an evolution of the Hubble parameter, is obtained in [27]. Other reviews on the reconstruction of dark energy and modified gravity can be found in [28,29]. In this work, we consider a sufficiently general form for $f(R, T)$, associating it with Barrow's holographic dark energy in a manner that facilitates plotting and estimation of the terms within the $f(R, T)$ model. In this context, we investigate the reconstruction of $f(R, T)$ theory based on the Barrow holographic dark energy, considering three different infrared cutoffs.

This paper is organized as follows. In Sect. 2, we introduce the Barrow holographic dark energy, derive the Friedmann equation, and calculate the equation of state parameter and the density parameter for three different infrared cutoffs: the Hubble horizon, the future event horizon, and the Granda–Oliveros cutoff. In Sect. 3, we present $f(R, T)$ gravity, derive an equation of state parameter, and develop a reconstruction of $f(R, T)$ theory considering the Barrow holographic dark energy. We explore this reconstruction for the Hubble horizon, the future event horizon, and the Granda–Oliveros cutoff, discussing some numerical results. Finally, in Sect. 4, we provide some concluding remarks.

2 Holographic dark energy

In this section, the holographic dark energy scenario is briefly presented. Holographic dark energy is an interesting construct that describes dark energy, originating from the holographic principle [2,3]. In this context, Barrow holographic dark energy is introduced [8]. The state parameter and the density parameter will be investigated for different infrared (IR) cutoffs, including the Hubble horizon, the future event horizon, and the Granda–Oliveros cutoff.

Let us consider an isotropic and homogeneous universe with spacetime geometry defined by the flat Friedmann–Robertson–Walker (FRW) metric, given as

$$ds^2 = -dt^2 + a(t)^2(dr^2 + r^2 d\Omega^2), \tag{1}$$

where $a(t)$ is the scale factor. This universe is filled with a perfect fluid whose energy-momentum tensor is given by

$$T_{\mu\nu} = (\rho + p)u_\mu u_\nu + p g_{\mu\nu} \tag{2}$$

with ρ, p and u_μ being the energy density, pressure and the four-velocity of the fluid, respectively. With these ingredients, the Einstein field equations lead to the Friedmann equation

$$3H^2 = \kappa(\rho_m + \rho_{DE}), \tag{3}$$

where ρ_m and ρ_{DE} denote the energy density of dark matter (DM) and dark energy (DE), respectively. We assume that DM and DE do not interact with each other. Therefore, they satisfy the standard conservation equations, i.e.,

$$\dot{\rho}_m + 3H\rho_m = 0, \tag{4}$$

$$\dot{\rho}_{DE} + 3H(1 + \omega_{DE})\rho_{DE} = 0 \tag{5}$$

with $\omega_{DE} = p_{DE}/\rho_{DE}$ being the equation of state (EoS) parameter of DE.

Taking the time derivative of Eq. (3) and using Eqs. (4) and (5), we obtain

$$2\dot{H} = -\kappa(\rho_m + \rho_{DE} + \omega_{DE}\rho_{DE}). \tag{6}$$

Defining the density parameter as $\Omega_i \equiv \rho_i/\rho_c = \frac{\kappa\rho_i}{3H^2}$, where ρ_c is the critical energy density and $\kappa = 8\pi G$, Eq. (6) can be written as

$$\frac{\dot{H}}{H^2} = -\frac{3}{2}(1 + \omega_{DE}\Omega_{DE}). \tag{7}$$

It has been used that $\Omega_m + \Omega_{DE} = 1$.

Using this relation, it is possible to determine the state parameter and the density parameter given one or the other. We can find a solvable equation for the density parameter and differentiate it with respect to time (t), e-fold number ($\ln a$), redshift (z), or matter density. Then

$$\begin{aligned}
\frac{d\Omega(t)}{dt} &= H(\ln a)\frac{d\Omega(\ln a)}{d\ln a} \\
&= -H(z)(1 + z)\frac{d\Omega(z)}{dz} \\
&= -3H(\rho_m)\rho_m\frac{d\Omega(\rho_m)}{d\rho_m}.
\end{aligned} \tag{8}$$

In a general form, it can be expressed as

$$\frac{d\Omega}{dt} = \frac{d\ln a}{dt}\frac{d\Omega}{d\ln a} = H\Omega'(\ln a). \tag{9}$$

From the definition of the density parameter, it becomes

$$H\Omega'_{DE}(\ln a) = \partial_t\left(\frac{\kappa\rho_{DE}}{3H^2}\right) = \frac{k}{3}(\dot{\rho}_{DE}H^{-2} - 2\rho_{DE}H^{-3}\dot{H}) \tag{10}$$

with a dot representing the time derivative and a prime denoting the derivative with respect to the function argument. This

relation can be solved for a given energy density, here taken from the holographic principle.

The holographic principle postulates that the description of a system can be based on its surface properties rather than its volume, suggesting that entropy is bounded to be proportional to the area of the boundary. As a result, the energy density, constrained by the entropy as $L^3 \rho_{DE}^{3/4} \leq S^{3/4}$, is also confined to the area, that is,

$$\rho_{DE} \leq \frac{B}{L^2}, \tag{11}$$

where B is a parameter to be defined, L is the infrared cutoff representing the longest distance of the system. We choose the value of ρ_{DE} that saturates the inequality.

In this study, we consider the Barrow holographic dark energy model [8]. Barrow demonstrated how the boundary area of a black hole can exhibit significantly different values when viewed as a fractal. In this scenario, the system's entropy becomes $S = S_{BH}^{1+\Delta/2}$, with Δ representing the intricacy of the surface, where $\Delta = 0$ indicates perfect smoothness and $\Delta = 1$ represents maximum complexity. From this entropy expression, we derive Barrow holographic dark energy given as

$$\rho_{DE} = \rho_{BHDE} = BL^{\Delta-2}. \tag{12}$$

It is possible to insert this energy density into Eq. (10), but finding its solution and the state parameter will necessitate defining an infrared cutoff for the holographic dark energy. Now, three different IR cutoffs will be considered.

2.1 Hubble horizon

In this subsection, the Hubble horizon cutoff is introduced [30–32], followed by an analysis of the cosmological behavior of the universe. The Hubble horizon cutoff is defined as $L = H^{-1}$. Then, the energy density of DE becomes

$$\rho_{DE} = BH^{2-\Delta}. \tag{13}$$

Taking its time derivative and using the energy conservation relation Eq. (5), we obtain

$$\omega_{DE} = -\frac{(2-\Delta)\dot{H}}{3H^2} - 1. \tag{14}$$

From Eq. (7), the state parameter can be expressed as a function of the density parameter, i.e.,

$$\omega_{DE} = \frac{\Delta}{(2-\Delta)\Omega_{DE} - 2}. \tag{15}$$

Considering Eqs. (10) and (7), the following relation for the density parameter is obtained

$$\Omega'_{DE} = 3\Delta\Omega_{DE}\left(\frac{\Omega_{DE} - 1}{(2-\Delta)\Omega_{DE} - 2}\right). \tag{16}$$

From here, we can numerically find the solution. We can also change the dependency of the density parameter to ρ_m, resulting in the following differential equation:

$$\Omega'_{DE} = -\frac{\Delta\Omega_{DE}}{\rho_m}\left(\frac{\Omega_{DE} - 1}{(2-\Delta)\Omega_{DE} - 2}\right). \tag{17}$$

This will later allow the calculation of a solution for $f(R, T)$ models in scenarios involving dust matter. In Fig. 1, the numerical solutions for the density parameter and state parameter as a function of energy density are shown, considering the Hubble horizon as the IR cutoff. In this context, our results indicate that an accelerating expansion of the universe is permitted when the Hubble cutoff is considered. Furthermore, for the Hubble cutoff, acceleration can only be achieved with non-zero delta Δ values. In all these scenarios, exponential expansion occurs in the distant future. Delta values below 2/3 lead to a transition from deceleration to acceleration at some point in the past.

2.2 Future event horizon

Since the Hubble radius is not a suitable event horizon given that we can observe objects beyond it, many prefer to explore holographic theories using other distances, such as the future event horizon [33]. In this case, the infrared cutoff is defined as

$$L = R_h = a(t)\int_t^\infty \frac{dt}{a(t)} \tag{18}$$

with $\dot{R}_h = HR_h - 1$.

Using the future event horizon as the infrared cutoff, the Barrow holographic dark energy density becomes $\rho_{DE} = BR_h^{\Delta-2}$, and its time derivative is given by
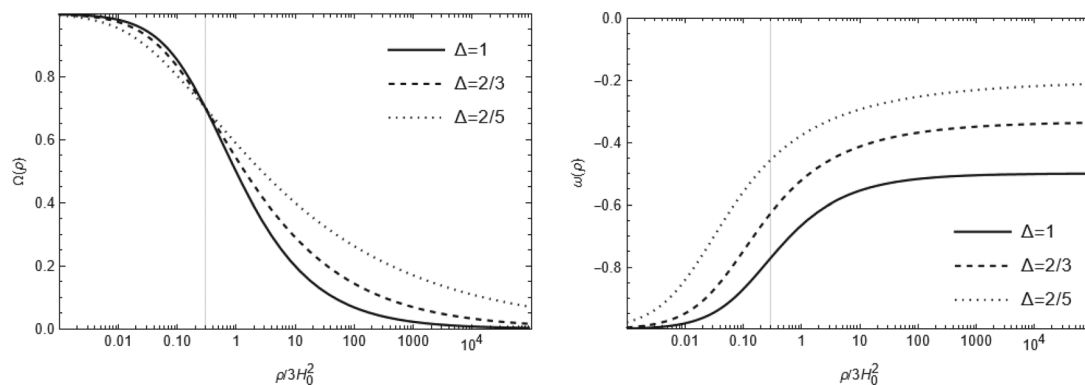
$$\dot{\rho}_{DE} = \rho_{DE}(\Delta - 2)H(1 - F), \tag{19}$$

where

$$F = \left(\frac{3\Omega_{DE}H^\Delta}{\kappa B}\right)^{\frac{1}{2-\Delta}} \tag{20}$$

with $\Omega_{DE} = \frac{\kappa}{3H^2}\rho_{DE}$. From the energy conservation equation, i.e. $\dot{\rho}_{DE} + 3H(1 + \omega_{DE})\rho_{DE} = 0$, and using Eq. (19), the EoS parameter is written as

$$\omega_{DE} = -1 - \frac{\Delta - 2}{3}(1 - F). \tag{21}$$

Fig. 1 Plot of numeric solutions for the density parameter (left) and EoS parameter (right), using $\Omega_{DE0} = 0.7$, with different values of the Δ parameter. The vertical lines in the plots represent $\rho = \rho_{m0}$, i.e. the present time

Substituting these ingredients into Eq. (10) and using Eq. (7), the differential equation for the density parameter is given as

$$\Omega'_{DE} = \Omega_{DE}(1 - \Omega_{DE})[1 - F(\Delta - 2) + \Delta]. \tag{22}$$

To accurately calculate the above equation, it is necessary to address the Hubble parameter within F. This can be achieved by using the Friedmann equation and expressing it as follows:

$$\begin{aligned}
H^2 &= \frac{\kappa}{3}(\rho_{m0}(1+z)^3 + \rho_{DE}) \\
&= H_0^2 \Omega_{m0}(1+z)^3 + H^2 \Omega_{DE} \\
&= H_0^2 \frac{1 - \Omega_{DE0}}{1 - \Omega_{DE}}(1+z)^3,
\end{aligned} \tag{23}$$

where the suffixes 0, such as $m0$ and $DE0$ refer to values at the current epoch.

The numeric solutions for Ω_{DE} and ω_{DE}, considering the future event horizon as the infrared cutoff, are shown in Fig. 2. For the future event horizon cutoff, acceleration always occurs regardless of the value of delta. In contrast to the Hubble case, this parameter significantly influences the behavior in the distant future.

It is important to note that employing the method of first solving $H(z)$, differentiating the Friedmann equation, and then calculating the density and EoS parameter yields the same results as presented above.

2.3 Granda–Oliveros cutoff

The future event horizon represents a potential causality violation, since its calculation requires knowledge of the scale factor value in the future [34]. Granda and Oliveros proposed a purely mathematical approach as a cutoff to avoid this issue [35,36]. The Barrow holographic dark energy with the Granda–Oliveros (GO) cutoff has been investigated in [37]. With this cutoff, $L = \left(\alpha H^2 + \beta \dot{H}\right)^{-1/2}$, we can read-

ily determine the energy density of dark energy as follows

$$\rho_{DE} = B\left(\alpha H^2 + \beta \dot{H}\right)^{\frac{2-\Delta}{2}} \tag{24}$$

which leads to

$$\frac{\dot{H}}{H^2} = \frac{1}{\beta}\left((\Omega_{DE}H^\Delta)^{\frac{2}{2-\Delta}} - \alpha\right) \equiv F. \tag{25}$$

Here, $B = 3m_p^2$ has been chosen, and this expression is denoted as F for simplicity. Inserting this result into Eq. (10) and substituting $\dot{\rho}_{DE} = 3m_p^2(2H\dot{H} + 3H^3\Omega_m)$ from Friedmann and energy conservation equations, we obtain

$$\Omega'_{DE} = (1 - \Omega_{DE})(3 + 2F). \tag{26}$$

Using Eq. (7) the EoS parameter is given as

$$\omega_{DE} = -\frac{2F + 3}{3\Omega_{DE}}. \tag{27}$$

Similar to the previous cases, the density parameter and EoS parameter are numerically determined, as shown in Fig. 3. The GO cutoff preserves the characteristics of the future event horizon case for both the current and distant future epochs. However, in all scenarios, it induces the transition from deceleration to acceleration more prominently than the Hubble case.

3 Reconstructing an $f(R, T)$ model from Barrow holographic dark energy

In this section, the main objective is to reconstruct the $f(R, T)$ gravity within the Barrow holographic dark energy model. First, a brief introduction to the standard $f(R, T)$
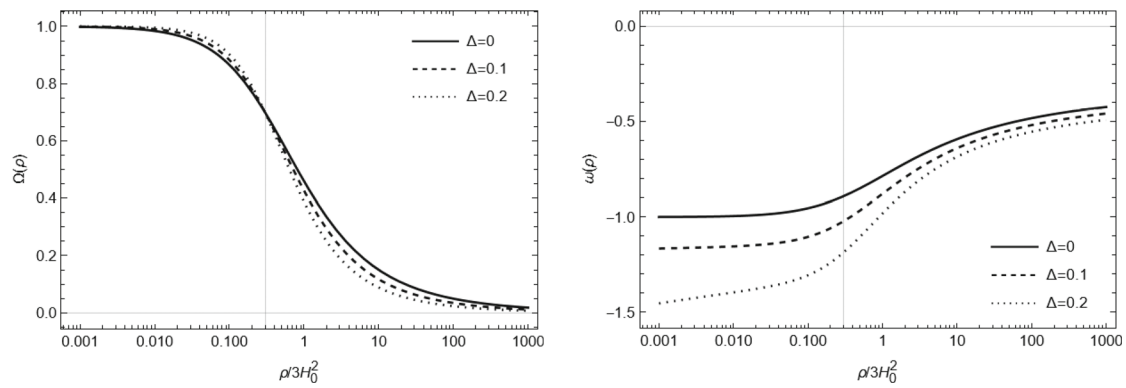
Fig. 2 Plot of numeric solutions for the density parameter (left) and EoS parameter (right), using $\Omega_{DE0} = 0.7$ and $H_0 = 67$, with different values of Δ
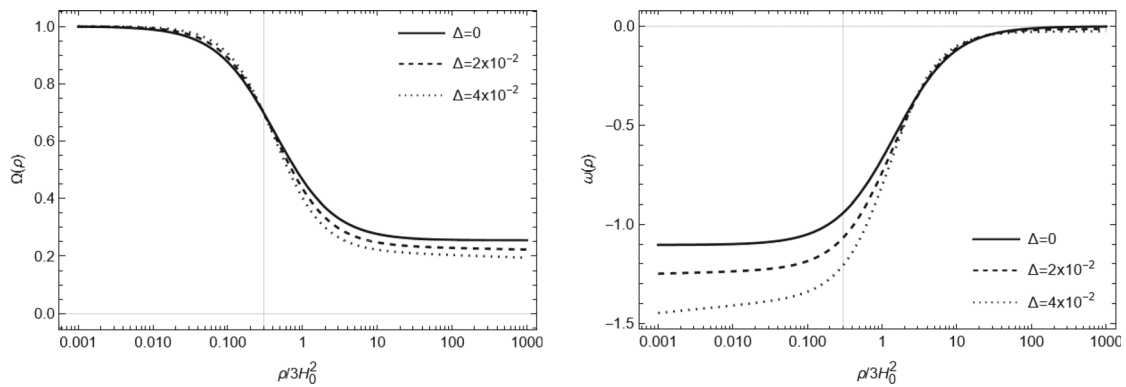
Fig. 3 Plot of numeric solutions for the density parameter (left) and EoS parameter (right), using $\Omega_{DE0} = 0.7$, $H_0 = 67$, $\alpha = 0.93$ and $\beta = 0.45$, with different values of Δ

gravity is provided. Then, it is proposed to reconstruct the theory considering different event horizons.

This gravitational theory consists of a generalization of the Einstein–Hilbert action of general relativity. In this case, the Ricci scalar R in the general relativity action is replaced by a function f that depends on both the Ricci scalar R and the trace of the energy–momentum tensor T. The action that describes $f(R, T)$ gravity is given by

$$S = \int [f(R, T) + \mathcal{L}_m] \sqrt{-g} d^4 x, \tag{28}$$

where g represents the determinant of the metric and $\mathcal{L}_m$ is the Lagrangian describing the matter content. A review on $f(R, T)$ gravity can be found in [38,39]. Several studies have been developed considering this theory of gravity. For example, reconstructions of cosmological models within $f(R, T)$ theory have been investigated in [25,40,41], while perturbations, constraints, and the Palatini formulation are presented in [42–44].

Varying the action (28) with respect to the metric and considering a perfect fluid as the matter content, with a Lagrangian defined by $\mathcal{L}_m = -p$, the field equations are

given as

$$
\begin{aligned}
&f_R(R, T)R_{\mu\nu} - \frac{1}{2}f(R, T)g_{\mu\nu} \\
&\quad + (g_{\mu\nu}\Box - \nabla_\mu \nabla_\nu) f_R(R, T) \\
&= T_{\mu\nu} + f_T(R, T)T_{\mu\nu} + p f_T(R, T)g_{\mu\nu},
\end{aligned}
\tag{29}
$$

where $f_R(R, T) = \frac{\partial f(R,T)}{\partial R}$, $f_T(R, T) = \frac{\partial f(R,T)}{\partial T}$ and $T_{\mu\nu}$ is the energy-momentum tensor which is defined as

$$T_{\mu\nu} = -\frac{2}{\sqrt{-g}} \frac{\delta(\sqrt{-g}\mathcal{L}_m)}{\delta g^{\mu\nu}}. \tag{30}$$

Here, let's choose one of the simplest models of $f(R, T)$ gravity, which consists of the usual general relativity term, the Ricci scalar R, plus an $f(T)$ correction, i.e., $f(R, T) = R + 2f(T)$. Then, the field equations become

$$R_{\mu\nu} - \frac{1}{2}Rg_{\mu\nu} = T_{\mu\nu} + 2f_T(T)T_{\mu\nu} + 2p f_T(T)g_{\mu\nu} + f(T)g_{\mu\nu}. \tag{31}$$

Taking an isotropic and homogeneous universe described by the FRW metric Eq. (1) filled with a perfect fluid whose energy-momentum tensor is given in Eq. (2), leads to the
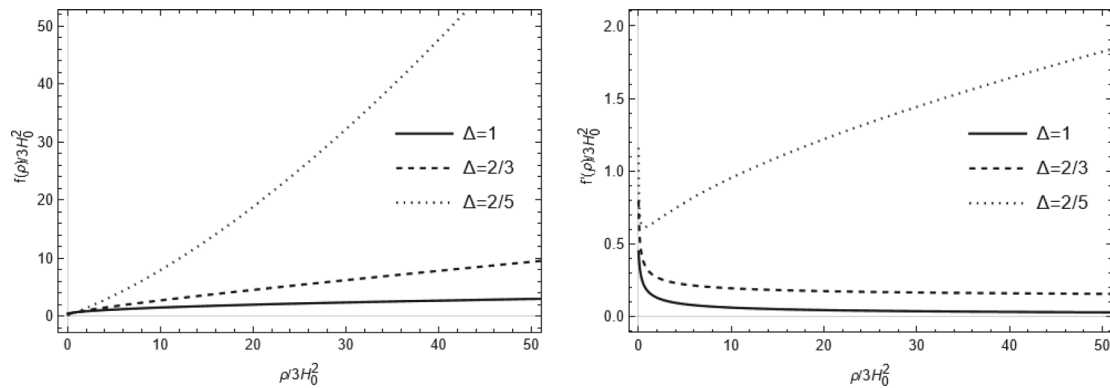
Fig. 4 Plot of numeric solutions for $f(\rho_m)$ (left) and its derivative (right), using $\Omega_{DE0} = 0.7$

modified Friedmann equations

$$3H^2 = \rho + 2(\rho + p)f_T(T) + f(T) \equiv \rho + \rho_{f(T)} \tag{32}$$

$$-2\dot{H} - 3H^2 = p - f(T) \equiv p + p_{f(T)}. \tag{33}$$

Here, $\rho_{f(T)}$ and $p_{f(T)}$ represent the modified energy density and pressure associated with the $f(T)$ contribution. These quantities are defined as follows

$$\rho_{f(T)} = 2(\rho + p)f_T(T) + f(T), \tag{34}$$

$$p_{f(T)} = -f(T). \tag{35}$$

It is important to note that from these elements, the equation of state parameter induced by the function $f(T)$ is defined as

$$\omega_{f(T)} \equiv \frac{p_{f(T)}}{\rho_{f(T)}} = -\frac{f(T)}{2(\rho + p)f_T + f(T)} \tag{36}$$

and the deceleration parameter is given by

$$q \equiv -1 - \frac{\dot{H}}{H^2} = \frac{\rho + 3p + (\rho + p)2f_T - 2f(T)}{2\rho + 4(\rho + p)f_T + 2f(T)}.$$

It is important to highlight that the interpretation of the deceleration parameter aligns with that of the state parameter.

With these results, the main objective now is to reconstruct the $f(R, T)$ theory from Barrow holographic dark energy. For this, let's assume that the equation of state (EoS) parameter given in Eq. (36) is equal to the EoS parameter of dark energy (ω_{DE}) in a context where the matter content is dust. The trace of the energy-momentum tensor for this matter content is $T = \rho$. Then, by taking $\omega_{f(T)} = \omega_{DE}$, we obtain

$$f_\rho = -\frac{f(\rho)}{2\rho}\left(1 + \frac{1}{\omega_{DE}}\right). \tag{37}$$

It is worth noting that in the specific case of $\omega_{DE} = -1$, this derivative vanishes, leading to a constant $f(\rho)$. Substituting this into Eq. (32) recovers the well-known de Sitter evolution.
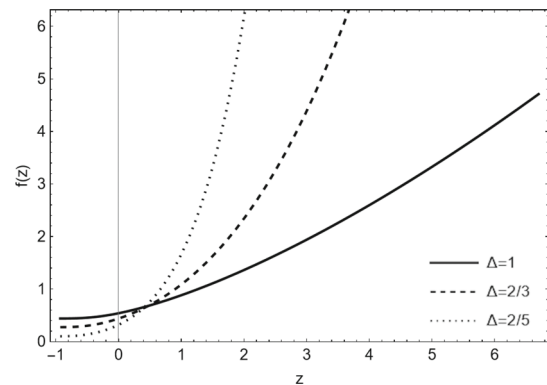
Fig. 5 Plot of numeric solution for $f(z)$, using $\Omega_{DE0} = 0.7$

To correctly calculate the solution of $f(\rho)$, we need an initial condition. From the modified Friedmann equations (32), we find

$$f_\rho(\rho_0) = \frac{3H_0^2 \Omega_{DE0}}{2\rho_0} - \frac{f(\rho_0)}{2\rho_0}. \tag{38}$$

Using this result in Eq. (37) at the current time leads to

$$f(\rho_0) = -3H_0^2 \Omega_{DE0}\omega_{DE0}. \tag{39}$$

In order to continue the reconstruction of $f(R, T)$ theory using Eq. (37), different IR cutoffs will be considered, namely the Hubble horizon, the future event horizon, and the Granda–Oliveros cutoff.

3.1 Hubble horizon

As a first case, the Hubble cutoff is considered. For this cutoff, the EoS parameter is given in Eq. (15). Using this result, Eq. (37) becomes

$$f_\rho = -\frac{f(\rho)}{2\rho}\left(1 + \frac{(2 - \Delta)\Omega_{DE} - 2}{\Delta}\right), \tag{40}$$
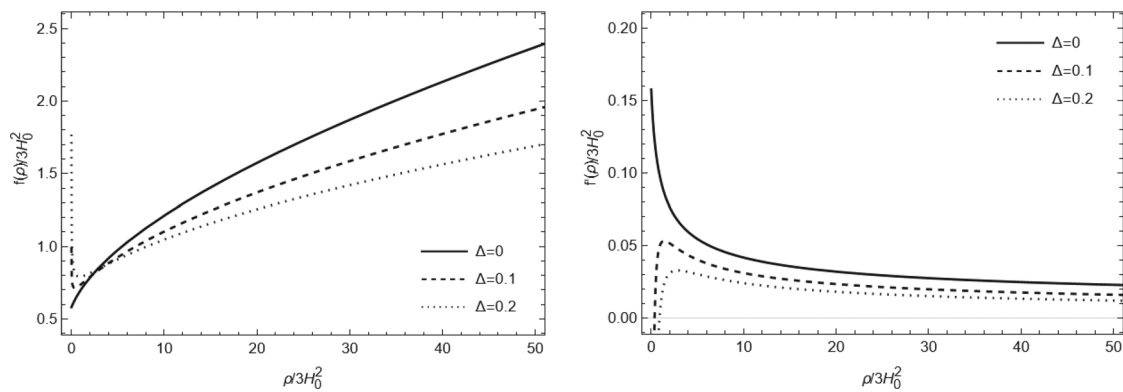
Fig. 6 Plot of numeric solutions for $f(\rho_m)$ (left) and its derivative (right), using $\Omega_{DE0} = 0.7$, $H_0 = 67$

with initial condition given by

$$f(\rho_{m0}) = -\frac{3H_0^2 \Omega_{DE0} \Delta}{(2-\Delta)\Omega_{DE0} - 2}. \tag{41}$$

We can immediately see that for $\Delta = 0$, it is not possible to compute $f(\rho)$. However, for $\Delta = 2$, we obtain the cosmological constant scenario with $f(\rho) = \rho_{DE0}$. For other values of Δ, using the results of Ω, we calculate the solution for $f(\rho_m)$. This solution for different values of Δ is shown in Figs. 4 and 5.

At first glance, the early component of the function $(f_E(\rho))$ appears to follow a power law, i.e.,

$$f_E(\rho) = \alpha \rho^{g(\Delta)}, \tag{42}$$

where α is a constant and $g(\Delta)$ a function of Δ. For Δ values close to zero, the slope of the function increases dramatically and begins to resemble an exponential.

Values of Δ were chosen based on their effect on the function in the past. In this case, $f(\rho)$ appears to be a square root for $\Delta = 1$, linear for $\Delta = 2/3$, and quadratic for $\Delta = 2/5$. This can also be verified by solving the equations for $\Omega_{DE} \ll 1$, providing a hint of the form the function should take. In the far future ($\Omega_{DE} \approx 1$), the function becomes constant. But in all situations, there is a change in behavior from the near past to the future, with a significant positive change in the slope of f in the future and its derivative always being positive. This indicates the presence of other term(s) in the $f(\rho)$ function that dominate at lower ρ_m values. As of now, our best guess for the late component $(f_L(\rho))$ is something like

$$f_L(\rho) = a \ln(\rho^{h(\Delta)} + c) \quad \text{or} \quad f_L(\rho) = b \, \rho^{h(\Delta)}, \tag{43}$$

where a, b and c are constants and $0 < h(\Delta) < 1$.

In the next subsection, we investigate $f(\rho)$ considering a different horizon cutoff, thus reconstructing the $f(R, T)$ theory from a different perspective.
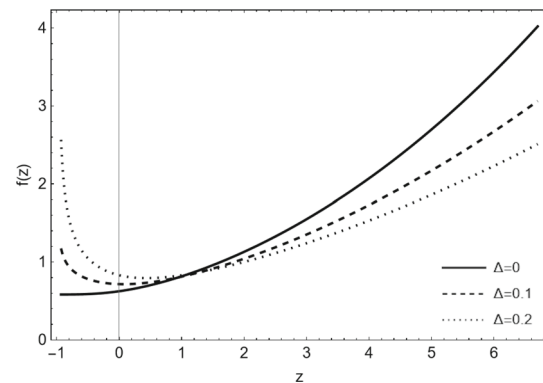
Fig. 7 Plot of numeric solution for $f(z)$, using $\Omega_{DE0} = 0.7$, $H_0 = 67$

3.2 Future event horizon

Here, the future event horizon cutoff is considered. Using the EoS parameter given in Eq. (21), we can express Eq. (37), which determines the function f_ρ, as

$$f_\rho = -\frac{f(\rho)}{2\rho}\left(1 - \frac{3}{3 + (\Delta - 2)(1 - F)}\right). \tag{44}$$

The initial condition is given by

$$f(\rho_{m0}) = -3H_0^2 \Omega_{DE0}\left(-1 - \frac{\Delta - 2}{3}(1 - F_0)\right). \tag{45}$$

Using the results of Ω, we calculate the solution for $f(\rho_m)$. These results are shown in Figs. 6 and 7, considering different values of Δ.

There is clearly a functional transition to $\Delta \neq 0$. In the past, it behaves as a power law, $f_E(\rho) \propto \rho^{g(\Delta)}$, with $g(\Delta) < 1$ inversely proportional to Δ. Toward the present and future, it transitions to $f_L(\rho) \propto \rho^{-h(\Delta)}$, with $h(\Delta)$ also inversely proportional to Δ and disappearing into $\Delta = 0$. The first derivative $f'(\rho)$ appears to be a function like

$$f'(\rho) \propto \rho^{-g'(\Delta)} - \rho^{-h'(\Delta)} \tag{46}$$
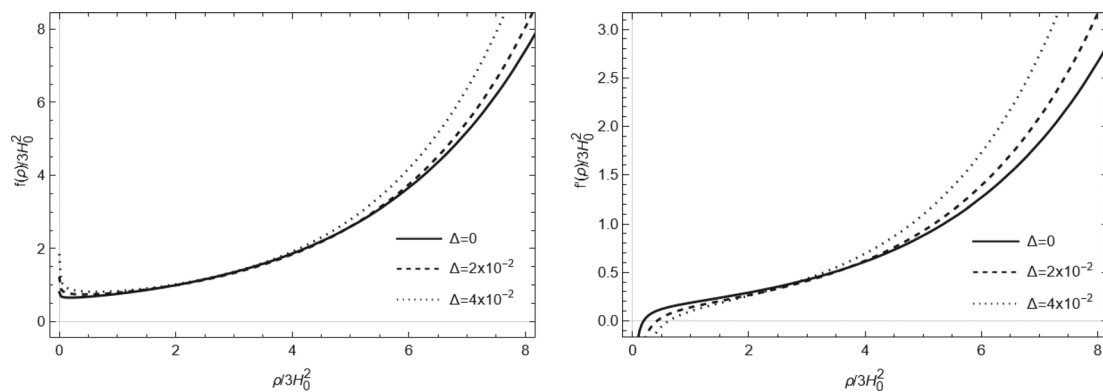
Fig. 8 Plot of numeric solutions for $f(\rho_m)$ (left) and its derivative (right), using $\Omega_{DE0} = 0.7$, $H_0 = 67$, $\alpha = 0.93$ and $\beta = 0.45$
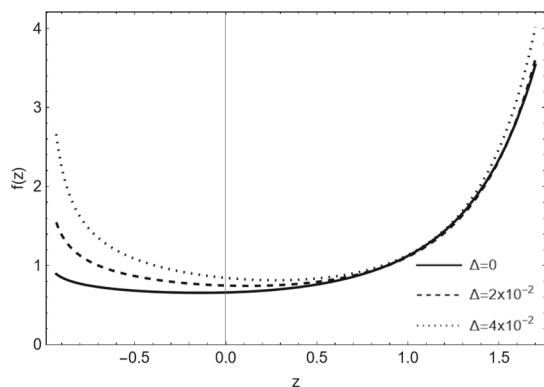
Fig. 9 Plot of numeric solution for $f(z)$, using $\Omega_{DE0} = 0.7$, $H_0 = 67$, $\alpha = 0.93$ and $\beta = 0.45$

where $h'(\Delta) > g'(\Delta)$, and $h'(\Delta)$ vanishes for $\Delta = 0$. This result is largely similar to the one obtained with the Hubble cutoff during the early stages of expansion but deviates significantly as we approach the current era.

3.3 Granda–Oliveros cutoff

The third IR cutoff being considered is the Granda–Oliveros cutoff. For this cutoff, the EoS parameter is defined in (27). Then, for this case, Eq. (37) is expressed as

$$f_\rho = -\frac{f(\rho)}{2\rho}\left(1 - \frac{3\Omega_{DE}}{3 + 2F}\right) \tag{47}$$

and its initial condition is

$$f(\rho_{m0}) = -3H_0^2 \Omega_{DE0}\left(-\frac{3 + 2F_0}{3\Omega_{DE0}}\right) \tag{48}$$

with $F_0 = \frac{1}{\beta}\left((\Omega_{DE0}H_0^\Delta)^{\frac{2}{2-\Delta}} - \alpha\right)$. Using the results of Ω, the solution for $f(\rho_m)$ is found, as exhibited in Figs. 8 and 9.

From the function and its derivatives, we can observe that it is exponential in the past for any values of Δ, given by

$$f(\rho) \propto e^{g(\Delta)\rho} \quad \text{or} \quad f(\rho) \propto e^{\rho^{g(\Delta)}}, \tag{49}$$

where $g(\Delta) \propto \Delta$. There is a transition in the present and future that appears to become an inverse power law, $f(\rho) \propto \rho^{-g(\Delta)}$, with $g(\Delta) \propto 1/\Delta$, similar to the one proposed for the future event horizon. These approximated solutions have been studied in the context of $f(R, T)$ and $f(R, L_m)$ gravity [45,46].

For both the future event horizon and Granda–Oliveros cutoffs, we obtain $f(\rho)$ solutions where its influence in later eras is significantly larger than ρ_m, implying that the Hubble parameter, as derived from the modified Friedmann equations (32), will resemble these solutions. This behavior aligns with the expected trends observed in the state parameters, as discussed in the previous section, showing a transition from power-law expansion to exponential growth and beyond.

4 Conclusion

The late-time accelerated expansion of the universe remains one of the most challenging problems of the last few decades. To address this problem, various attempts have been made. These include the proposal of alternative gravity theories and the consideration of exotic forms of matter or energy. This work investigates a dark energy model based on the holographic principle, known as Barrow holographic dark energy. In this context, we calculate the equation of state parameter and the density parameter of dark energy under three different cutoff conditions: the Hubble horizon, the future event horizon, and the Granda–Oliveros cutoff, with the latter exhibiting the expected behavior while avoiding some of the theoretical issues associated with the other two. Our findings reveal distinct scenarios that describe the accelerated expansion of the universe in the present epoch. Additionally, the Barrow

holographic dark energy model is utilized to reconstruct the $f(R, T)$ theory. This reconstruction is analyzed across various infrared cutoffs. The results demonstrate that it is possible to determine the function $f(\rho)$ from the equation of state parameter associated with certain infrared cutoffs. The analysis presented here focuses on a specific $f(R, T)$ model, namely $f(R, T) = R + 2f(T)$, under the assumption that the universe's matter content is dust. We obtain numerical results and utilize them to estimate the behavior of the function $f(\rho)$ across various periods of the universe's evolution. Moreover, our results, which demonstrate the reconstruction of a $f(R, T)$ theory, align with observational data indicating a late acceleration of the universe's expansion.

Data Availability Statement My manuscript has no associated data. No data are available because of the nature of the research. This publication is theoretical work that does not require supporting research data.]

Code Availability Statement My manuscript has no associated code/software. [Authors' comment: Code/Software sharing not applicable to this article as no code/software was generated or analysed during the current study.]

References

1. C.M. Will, The confrontation between general relativity and experiment. Living Rev. Relativ. **17**, 4 (2014). https://doi.org/10.12942/lrr-2014-4
2. L. Susskind, The world as a hologram. J. Math. Phys. **36**, 6377 (1995). https://doi.org/10.1063/1.531249
3. R. Bousso, The holographic principle. Rev. Mod. Phys. **74**, 825 (2002). https://doi.org/10.1103/RevModPhys.74.825
4. J.D. Bekenstein, Black holes and the second law. Lett. Nuovo Cim. **4**, 737 (1972). https://doi.org/10.1007/BF02757029
5. J.D. Bekenstein, Black holes and entropy. Phys. Rev. D **7**, 2333 (1973). https://doi.org/10.1103/PhysRevD.7.2333
6. S.W. Hawking, Black hole explosions? Nature **248**, 30 (1974). https://doi.org/10.1038/248030a0
7. S.W. Hawking, Black holes and thermodynamics. Phys. Rev. D **13**, 191 (1976). https://doi.org/10.1103/PhysRevD.13.191
8. J.D. Barrow, The area of a rough black hole. Phys. Lett. B **808**, 135643 (2020). https://doi.org/10.1016/j.physletb.2020.135643
9. E.N. Saridakis, Barrow holographic dark energy. Phys. Rev. D **102**, 123525 (2020). https://doi.org/10.1103/PhysRevD.102.123525
10. S. Nojiri, S.D. Odintsov, T. Paul, Barrow entropic dark energy: a member of generalized holographic dark energy family. Phys. Lett. B **825**, 136844 (2022). https://doi.org/10.1016/j.physletb.2021.136844
11. J.D. Barrow, S. Basilakos, E.N. Saridakis, Big bang nucleosynthesis constraints on Barrow entropy. Phys. Lett. B **815**, 136134 (2021). https://doi.org/10.1016/j.physletb.2021.136134
12. F.K. Anagnostopoulos, S. Basilakos, E.N. Saridakis, Observational constraints on Barrow holographic dark energy. Eur. Phys. J. C **80**, 826 (2020). https://doi.org/10.1140/epjc/s10052-020-8360-5
13. M.A. Zadeh, A. Sheykhi, H. Moradpour, Note on Tsallis holographic dark energy. Eur. Phys. J. C **78**, 940 (2018). https://doi.org/10.1140/epjc/s10052-018-6427-3
14. E.N. Saridakis, Modified cosmology through spacetime thermodynamics and Barrow horizon entropy. J. Cosmol. Astropart. Phys. **2020**, 031 (2020). https://doi.org/10.1088/1475-7516/2020/07/031
15. E.N. Saridakis, S. Basilakos, The generalized second law of thermodynamics with Barrow entropy. Eur. Phys. J. C **81**, 644 (2021). https://doi.org/10.1140/epjc/s10052-021-09431-y
16. G.G. Luciano, J. Giné, Generalized interacting Barrow holographic dark energy: cosmological predictions and thermodynamic considerations. Phys. Dark Univ. **41**, 101256 (2023). https://doi.org/10.1016/j.dark.2023.101256
17. T.P. Sotiriou, V. Faraoni, $f(R)$ theories of gravity. Rev. Mod. Phys. **82**, 451 (2010). https://doi.org/10.1103/RevModPhys.82.451
18. T. Harko, F.S.N. Lobo, S. Nojiri, S.D. Odintsov, $f(R, T)$ gravity. Phys. Rev. D **84**, 024020 (2011). https://doi.org/10.1103/PhysRevD.84.024020
19. T. Harko, F.S.N. Lobo, Generalized curvature-matter couplings in modified gravity. Galaxies **2**, 410 (2014). https://doi.org/10.3390/galaxies2030410
20. S. Bhattacharjee, Big bang nucleosynthesis and entropy evolution in f(R, T) gravity. Eur. Phys. J. Plus **135**, 350 (2020). https://doi.org/10.1140/epjp/s13360-020-00361-4
21. J.K. Singh, A. Singh, G.K. Goswami, J. Jena, Dynamics of a parametrized dark energy model in f(R, T) gravity. Ann. Phys. **443**, 168958 (2022). https://doi.org/10.1016/j.aop.2022.168958
22. R. Nagpal, S.K.J. Pacif, Cosmological aspects of $f(R, T)$ gravity in a simple model with a parametrization of q. Eur. Phys. J. Plus **136**, 875 (2021). https://doi.org/10.1140/epjp/s13360-021-01877-z
23. H. Velten, T.R.P. Caramês, Cosmological inviability of $f(R, T)$ gravity. Phys. Rev. D **95**, 123536 (2017). https://doi.org/10.1103/PhysRevD.95.123536
24. H. Shabani, M. Farhoudi, Cosmological and solar system consequences of $f(R, T)$ gravity models. Phys. Rev. D **90**, 044031 (2014). https://doi.org/10.1103/PhysRevD.90.044031
25. M.J.S. Houndjo, O.F. Piattella, Reconstructing $f(R, T)$ gravity from holographic dark energy. Int. J. Mod. Phys. D **21**, 1250024 (2012). https://doi.org/10.1142/S0218271812500241
26. C. Tsallis, L.J.L. Cirto, Black hole thermodynamical entropy. Eur. Phys. J. C **73**, 2487 (2013). https://doi.org/10.1140/epjc/s10052-013-2487-6
27. M. Zubair, Q. Muneer, E. Gudekli, Thermodynamics and stability analysis of Tsallis holographic dark energy (THDE) models in $f(R, T)$ gravity. Ann. Phys. **445**, 169068 (2022). https://doi.org/10.1016/j.aop.2022.169068
28. V. Sahni, A. Starobinsky, Reconstructing dark energy. Int. J. Mod. Phys. D **15**, 2105 (2006). https://doi.org/10.1142/S0218271806009704

29. M.J.S. Houndjo, Reconstruction of $f(R, T)$ gravity describing matter dominated and accelerated phases. Int. J. Mod. Phys. D **21**, 1250003 (2012). https://doi.org/10.1142/S0218271812500034

30. S.D.H. Hsu, Entropy bounds and dark energy. Phys. Lett. B **594**, 13 (2004). https://doi.org/10.1016/j.physletb.2004.05.020

31. L. Xu, Holographic dark energy model with Hubble horizon as an IR cut-off. JCAP **09**, 016 (2009). https://doi.org/10.1088/1475-7516/2009/09/016

32. S. Srivastava, U.K. Sharma, Barrow holographic dark energy with Hubble horizon as IR cutoff. Int. J. Geom. Methods Mod. Phys. **18**, 2150014 (2021). https://doi.org/10.1142/S0219887821500146

33. H.M. Sadjadi, Particle vs. future event horizon in interacting holographic dark energy model. JCAP **07**, 026 (2007). https://doi.org/10.1088/1475-7516/2007/02/026

34. M. Li, A model of holographic dark energy. Phys. Lett. B **603**, 1 (2004). https://doi.org/10.1016/j.physletb.2004.10.014

35. L.N. Granda, A. Oliveros, Infrared cut-off proposal for the holographic density. Phys. Lett. B **669**, 275 (2008). https://doi.org/10.1016/j.physletb.2008.10.017

36. L.N. Granda, A. Oliveros, New infrared cut-off for the holographic scalar fields models of dark energy. Phys. Lett. B **671**, 199 (2009). https://doi.org/10.1016/j.physletb.2008.12.025

37. A. Oliveiros, M.A. Sabogal, M.A. Acero, Barrow holographic dark energy with Granda–Oliveros cutoff. Eur. Phys. J. Plus **137**, 783 (2022). https://doi.org/10.1140/epjp/s13360-022-02994-z

38. T. Harko, F.S.N. Lobo, S. Nojiri, S.D. Odintsov, $f(R, T)$ gravity. Phys. Rev. D **84**, 024020 (2011). https://doi.org/10.1103/PhysRevD.84.024020

39. R. Myrzakulov, FRW cosmology in $f(R, T)$ gravity. Eur. Phys. J. C **72**, 2203 (2012). https://doi.org/10.1140/epjc/s10052-012-2203-y

40. M. Jamil, D. Momeni, M. Raza, R. Myrzakulov, Reconstruction of some cosmological models in $f(R, T)$ gravity. Eur. Phys. J. C **72**, 1999 (2012). https://doi.org/10.1140/epjc/s10052-012-1999-9

41. M. Sharif, M. Zubair, Reconstruction and stability of $f(R, T)$ gravity with Ricci and modified Ricci dark energy. Astrophys. Space Sci. **349**, 529 (2014). https://doi.org/10.1007/s10509-013-1623-y

42. F.G. Alvarenga, A. de la Cruz-Dombriz, M.J.S. Houndjo, M.E. Rodrigues, D. Saez-Gomez, Dynamics of scalar perturbations in $f(R, T)$ gravity. Phys. Rev. D **87**, 103526 (2013). https://doi.org/10.1103/PhysRevD.87.103526

43. F.G. Alvarenga, M.J.S. Houndjo, A.V. Monwanou, J.B. Chabi Orou, Testing some $f(R, T)$ gravity models from energy conditions. J. Mod. Phys. **4**, 130 (2013). https://doi.org/10.4236/jmp.2013.41019

44. J. Wu, G. Li, T. Harko, S. Liang, Palatini formulation of $f(R, T)$ gravity theory, and its cosmological implications. Eur. Phys. J. C **78**, 430 (2018). https://doi.org/10.1140/epjc/s10052-018-5923-9

45. A.P. Jeakel, J.P. Silva, H. Velten, Revisiting $f(R, T)$ cosmologies. Phys. Dark Univ. **43**, 101401 (2024). https://doi.org/10.1016/j.dark.2023.101401

46. T. Harko, F.S.N. Lobo, $f(R, L_m)$ gravity. Eur. Phys. J. C **70**, 373–379 (2010). https://doi.org/10.1140/epjc/s10052-010-1467-3